



Article

Dendropanax morbifera Leveille Extract-Induced Alteration of Metabolic Profile in Whitening Effects

Ting Bu ^{1,2}, Dongwon Kim ^{3,*}  and Sooah Kim ^{1,*}

¹ Department of Environment Science & Biotechnology, Jeonju University, Jeonju 55069, Republic of Korea; biting2006@163.com

² College of Life Sciences & Technology, Longdong University, Qingyang 745000, China

³ Department of Bio-Pharmaceutical Engineering, College of Bio-Health Convergence, Dongseo University, Busan 47011, Republic of Korea

* Correspondence: dwkim@dongseo.ac.kr (D.K.); skim366@jj.ac.kr (S.K.); Tel.: +82-63-220-2384 (S.K.)

Abstract: This study aimed to evaluate the potential of *Dendropanax morbifera* Leveille (*D. morbifera*) extract as a natural melanin depigmentation agent to achieve skin whitening. Treating α -MSH-stimulated B16-F10 cells with the extract effectively inhibited melanin production and tyrosinase activity. The cellular metabolic profiles were analyzed to understand the mechanisms underlying the whitening-related metabolic processes. We identified 29 metabolites that were significantly altered in the α -MSH-stimulated B16-F10 cells. The melanin-synthesis-related pathways that were downregulated included phenylalanine, tyrosine, and tryptophan biosynthesis and phenylalanine metabolism. Simultaneously, alanine, aspartate, and glutamate metabolism; arginine and proline metabolism; arginine biosynthesis; butanoate metabolism; glutathione metabolism; and glyoxylate and dicarboxylate metabolism were upregulated. We found that the optimal extract concentration of 0.2 mg/mL showed the highest efficacy in reversing the alterations to the metabolite levels and metabolic pathways. Moreover, *D. morbifera* extract exerted low cytotoxicity and high efficacy in inhibiting melanin production. Thus, *D. morbifera* extract is a potential melanin inhibitor with application in the development of whitening cosmetics.

Keywords: *Dendropanax morbifera* Leveille extract; melanin inhibitor; skin whitening; α -MSH-stimulated B16-F10 cells; tyrosinase activity



Citation: Bu, T.; Kim, D.; Kim, S. *Dendropanax morbifera* Leveille Extract-Induced Alteration of Metabolic Profile in Whitening Effects. *Horticulturae* **2024**, *10*, 219. <https://doi.org/10.3390/horticulturae10030219>

Academic Editor: Pablo Luis B. Figueiredo

Received: 30 January 2024
Revised: 22 February 2024
Accepted: 23 February 2024
Published: 25 February 2024



Copyright: © 2024 by the authors. Licensee MDPI, Basel, Switzerland. This article is an open access article distributed under the terms and conditions of the Creative Commons Attribution (CC BY) license (<https://creativecommons.org/licenses/by/4.0/>).

1. Introduction

Understanding the intricacies of melanin synthesis is fundamental to understanding skin biology because melanin is pivotal in determining skin pigmentation and various physiological functions. In addition to its involvement in skin and hair coloration, melanin is a critical safeguard against harmful ultraviolet radiation and an active participant in the wound healing processes [1,2]. Recent studies have delved into specific molecular mechanisms and have revealed insights into the regulation of tyrosinase activity, which is a key enzyme in melanin synthesis [3,4]. The intricacies of melanogenesis-related signaling pathways, including the MAPK and cAMP pathways, have also been established, which has led to the discovery of potential candidate compounds to regulate melanin synthesis [5–7]. These possible candidates include antioxidants such as flavonoids and polyphenols [8,9], which have exhibited the ability to modulate key enzymatic processes and disrupt melanogenesis-associated signaling cascades [10,11].

Dendropanax morbifera Leveille is a deciduous tree species of the family Araliaceae and is endemic to Korea and Japan [12]. It is known as “Mokchae” in Korea and is used in traditional remedies for numerous diseases. Recently, increased attention has been focused on *D. morbifera* owing to its pharmacological attributes and potential as a reservoir of natural bioactive compounds [13–15].

D. morbifera possess a wide range of pharmacological properties, including antioxidant [14,16], anti-inflammatory [13], antidiabetic [17,18], anticancer [19], hepatoprotective, [20] neuroprotective, and immunomodulatory [21,22] activities. The biological characteristics of *D. morbifera* are linked to its bioactive constituents such as triterpenoids, phenolic acids, flavonoids, lignans, and polysaccharides, which are primarily found in high concentrations in the leaves, stem bark, and roots of the plant [21,23,24]. Hence, these components have been traditionally used in Korean medicine to treat various diseases, including respiratory diseases [25], rheumatoid arthritis [26], liver diseases [20,27], and cancer [19].

Recent studies have explored its potential impact on skin health with a specific focus on its anti-aging and anti-inflammatory properties. Notably, *D. morbifera* extract enhances the production of collagen and elastin in human skin fibroblasts [28,29] and reduces the expression of pro-inflammatory cytokines such as IL-6 and TNF- α [30,31], suggesting that *D. morbifera* holds promise for application in cosmetic and skincare products as an anti-aging and anti-inflammatory agent.

Our preliminary experiments proved that *D. morbifera* extract has a higher quantity of flavonoids and polyphenols than other natural products, indicating that *D. morbifera* extract may exert potential whitening effects. In the current study, we used metabolomics to explore the whitening effect of *D. morbifera* extract to gain a comprehensive insight into the associated metabolic changes and elucidate the relationship between the alteration of metabolic pathways and the whitening effect, particularly with regard to reducing intracellular melanin levels. Additionally, we aimed to obtain a metabolic profile to discover the essential metabolites that are associated with the whitening effect exerted by *D. morbifera* extract.

2. Materials and Methods

2.1. Extract Preparation

D. morbifera extract was prepared as described previously with some modifications [15]. Briefly, 1 g of *D. morbifera* was mixed with 50 mL of 40% methanol for 24 h and extracted at 90 °C for 2 h with shaking at 200 rpm. After the extract was cooled and concentrated using rotary evaporation, the concentrate was kept at −20 °C for 24 h and freeze-dried. The lyophilized powder was stored at −20 °C for later use.

2.2. Analysis of Total Phenols and Total Flavonoids

Total phenol content was determined using the method described by Chen [32]. Briefly, 16 μ L of the extract (1 mg/mL, lyophilized powder dissolved in distilled water) and 60 μ L of Folin phenol reagent were mixed at 25 °C for 5 min. Then, 60 μ L of 60 g L^{−1} of NaCO₃ was added, and the mixture was kept at 25 °C for 90 min. The absorbance of the mixture was determined at 725 nm (Multiskan SkyHigh, Thermo Fisher Scientific, Waltham, MA, USA). Total phenol content is expressed as milligrams of gallic acid equivalents per gram of dry weight (mg GAE g^{−1} DW^{−1}).

Total flavonoid content was determined by following a previously described method [33]. Briefly, 80 μ L of distilled water, 6 μ L of 5% NaNO₂, and 6 μ L of 10% AlCl₃ were mixed with 20 μ L of the extract (1 mg mL^{−1}, lyophilized powder dissolved in distilled water) for 6 min. Then, 80 μ L of 4% NaOH was added, and the mixture was incubated in the dark at 25 °C for 30 min. The absorbance was measured at 405 nm (Multiskan SkyHigh, Thermo Fisher Scientific, Waltham, MA, USA). The total flavonoid content is expressed as milligrams of quercetin equivalents per gram of dry weight (mg QE g^{−1} DW^{−1}).

2.3. Cell Culture

B16-F10 cells (murine skin melanoma cells) were purchased from ATCC (CRL-6475) and cultured in Dulbecco's Modified Eagle Medium (DMEM) supplemented with 10% fetal bovine serum (FBS) (Gibco, Grand Island, NY, USA) and 1% antibiotics (Penicillin

and Streptomycin, Gibco, Grand Island, NY, USA) at 37 °C in a humidified incubator with 5% CO₂.

2.4. Cell Viability Assay

B16-F10 cells were seeded into a 96-well plate at a density of 5×10^4 cells/well and cultured for 24 h. Then, the cells were treated with α -melanocyte-stimulating hormone (500 ng mL⁻¹) (α -MSH, Sigma-Aldrich, Israel) and different concentrations of the extract (final concentrations: 0, 0.1, 0.2, 0.3, 0.4, 0.5, and 0.6 mg mL⁻¹) for 48 h. Next, 10 μ L of MTT reagent (3-(4,5-dimethyl-thiazol-2-yl)-2,5-diphenyltetrazolium bromide) (MTT; Sigma-Aldrich, St Louis, MO, USA) was added to each well, and the plate was incubated for 4 h at 37 °C for formazan production. Next, the culture medium was removed, and the formazan crystals were dissolved using 300 μ L of dimethyl sulfoxide (DMSO). Finally, the absorbance of each well was measured at 570 nm using a microplate reader (Multiskan SkyHigh, ThermoFisher, Waltham, MA, USA). Once the absorbance values had been obtained for each well, the data were analyzed to calculate the percentage of cell viability relative to that of the control (no treatment).

2.5. Melanin Content Measurement

B16-F10 cells (3 mL/well) were seeded into a 6-well plate at a density of 1×10^5 cells/mL and cultured for 24 h. Next, the cells were treated with 500 ng mL⁻¹ of α -MSH and various concentrations of *D. morbifera* extract (final concentrations: 0, 0.1, 0.2, and 0.3 mg mL⁻¹) for an additional 48 h. The cells were harvested, washed twice with PBS, and lysed with 150 μ L of 1 N NaOH (containing 10% DMSO) at 80 °C for 1 h to release the melanin pigment. The lysates were centrifuged to remove any remaining debris (then transferred into a 96-well plate), and the absorbance of the supernatant was measured at 405 nm using a spectrophotometer.

2.6. Tyrosinase Activity Detection

B16-F10 cells (3 mL/well) were plated into a 6-well plate at 1×10^5 cells/mL and incubated overnight at 25 °C. Then, the cells were incubated with different concentrations of *D. morbifera* extract (final concentrations: 0, 0.1, 0.2, 0.3, 0.4, 0.5, and 0.6 mg mL⁻¹). For the positive control, α -MSH (500 ng mL⁻¹) was added to the cells for 48 h to stimulate melanin production. Then, the cells were harvested, rinsed twice with cold PBS, and lysed using 500 μ L of 1% TritonX-100 dissolved in PBS. The mixture was kept at -80 °C for 30 min, followed by incubation at 25 °C for an additional 30 min. After centrifuging the lysate at 18,600 rpm for 15 min at 4 °C, the protein concentration was measured using a BCA Kit (QuantiPro™, Sigma-Aldrich, St. Louis, MO, USA). The concentration was adjusted to 20 μ g/100 μ L with PBS, and 200 μ L of the mixture was added to 10 μ L of 2% L-DOPA (3-(3,4-Dihydroxyphenyl)-2,5,6-d3)-L-alanine; Sigma-Aldrich, USA), followed by incubation at 37 °C for 1 h. The absorbance was measured at 490 nm using a microplate reader (1550, Thermo Fisher, Waltham, MA, USA).

2.7. Sample Preparation for Metabolomics

B16-F10 cells (3 mL/well) were plated into a 6-well plate at a density of 1×10^5 cells/mL and cultured for 24 h. Then, the cells were treated with α -MSH (500 ng mL⁻¹) and various concentrations of *D. morbifera* extract (final concentrations: 0, 0.1, 0.2, and 0.3 mg mL⁻¹) for an additional 48 h. Next, the cells were washed thrice with cold PBS. Then, 1 mL of cold methanol was added for quenching, and the cells were gently scraped with a rubber spatula. The quenched cells were extracted with a solvent mixture of MeOH to CHCl₃ to H₂O (4:4:2.85, v/v/v) for 30 min and centrifuged at 17,000 rpm for 3 min at 4 °C. The supernatant was completely dried using a vacuum concentrator (N-BIOTEK, NB-503CIR, Bucheon, Gyeonggi, Republic of Korea). To derivatize the sample, 10 μ L of 40 mg mL⁻¹ methoxyamine hydrochloride dissolved in pyridine was added to the dried metabolite sample and incubated at 30 °C for 90 min. Subsequently, 45 μ L of MSTFA

(N-methyl-N-(trimethylsilyl) trifluoroacetamide; Sigma-Aldrich, Buchs, Switzerland) was added and incubated at 37 °C for 30 min.

2.8. GC-MS Detection and Data Processing

The analysis of the derivatized samples was performed using a GC-qMS instrument (Shimadzu QP2010 plus, Shimadzu, Tokyo, Japan) equipped with an autosampler (AOC-20i+s, Shimadzu, Tokyo, Japan) and a primary Rtx-5MS capillary column (Cat. No. 13623-6850, Restek, Bellefonte, PA, USA, 30 m × 0.25 mm × 0.25 µm). A split ratio of 1:50 was used for injecting 1 µL of the derivatized sample into the GC-MS system at 280 °C with helium as a carrier gas at a flow rate of 1.5 mL min⁻¹. The column temperature was initially held at 60 °C for 3 min, followed by a gradual increase to 220 °C at the rate of 5 °C min⁻¹ for 4 min and 320 °C at the rate of 10 °C min⁻¹ for 6 min.

During the experiment, the retention time, peak shape, and intensity of the chromatogram of quality control (QC) samples were monitored meticulously to ensure overall stability of the analytical platform [34]. A coefficient of variation (CV) of less than 30% indicates good stability. The acquired mass spectra data were converted to .FAD format; processed using AMDIS (Automated Mass Spectrometry Deconvolution and Recognition System) for peak alignment, noise removal, and retention time calibration; and matched with a personal standard library [35]. The .ELU format results were uploaded to <http://spectconnect.mit.edu> (accessed on 23 July 2023) to be processed using a method and software implementation that can detect components across samples without a reference library or manual curation [36]. Additionally, metabolites were identified by comparison with compounds in the National Institute of Standards and Technology (NIST) MS library.

After obtaining a data matrix with the peak area of metabolites and sample numbers on the coordinate axis, multivariate analysis was performed using SIMCA 14.1. Unsupervised principal component analysis (PCA) and supervised orthogonal partial least squares-discriminant analysis (OPLS-DA) were performed [37]. The differential metabolites were screened based on the Student's t-test and variable importance in projection (VIP) scores of the OPLS-DA model, and hierarchical cluster analysis (HCA) was performed using MultiExperiment Viewer (MeV, version 4.9; Dana-Farber Cancer Institute, Boston, MA, USA) with Pearson correlation and average linkage. Furthermore, pathway analysis of the differential metabolites was performed using MetaboAnalyst 5.0 (<https://www.metaboanalyst.ca/>; accessed on 2 September 2023). The Origin 2021 software (OriginLab, Northampton, MT, USA) was used for other data analyses.

3. Results and Discussion

3.1. Total Phenol and Total Flavonoid Concentrations

The total phenolic and total flavonoid content in *D. morbifera*, which was extracted with 40% methanol (solid-to-liquid ratio, 1:50) at 90 °C for 2 h, was 95.2 ± 3.15 mg GAE g⁻¹ (gallic acid equivalents) and 79.75 ± 3.47 mg QE g⁻¹ (quercetin equivalents), respectively (Table 1).

Table 1. Total phenol and total flavonoid content in *Dendropanax morbifera* Leveille extract.

Sample	<i>Dendropanax morbifera</i> Leveille Extract
Total phenolic content (mg GAE g ⁻¹)	95.20 ± 3.15
Total flavonoid content (mg QE g ⁻¹)	79.75 ± 3.47

Total phenolic and flavonoid concentrations from other plants such as *Baphia nitida* (11.18 ± 0.30 mg GAE g⁻¹ and 36.35 ± 0.17 mg QE g⁻¹), *Crotolaria retusa* (15.00 ± 0.00 mg GAE g⁻¹ and 10.33 ± 0.00 mg QE g⁻¹), and *Mussaenda afzelii* (11.67 ± 0.09 mg GAE g⁻¹ and 0.37 ± 0.00 mg QE g⁻¹) were relatively lower than those from *D. morbifera* extract, indicating that *D. morbifera* extract may be a strong free radical scavenger [38].

3.2. Whitening Effects of *D. morbifera* Extract

As polyphenols and flavonoids can potentially inhibit melanin synthesis in the skin [10,11], the abundant presence of polyphenols and flavonoids in *D. morbifera* extract suggests the possibility of a potential whitening effect. Thus, we evaluated the whitening effect of *D. morbifera* extract on B16-F10 cells. Treatment of B16-F10 cells with $5 \times 10^{-5} \mu\text{g mL}^{-1}$ α -MSH and approximately 0.1 to 0.6 mg mL^{-1} of *D. morbifera* extract decreased cell viability as extract concentration increased; however, cell viability remained >85% in all treatments compared with that of the control. Moreover, at concentrations <0.2 mg mL^{-1} , the extract exerted no effect on B16-F10 cell viability ($p > 0.05$). Therefore, *D. morbifera* extract showed low toxicity (Figure 1a).

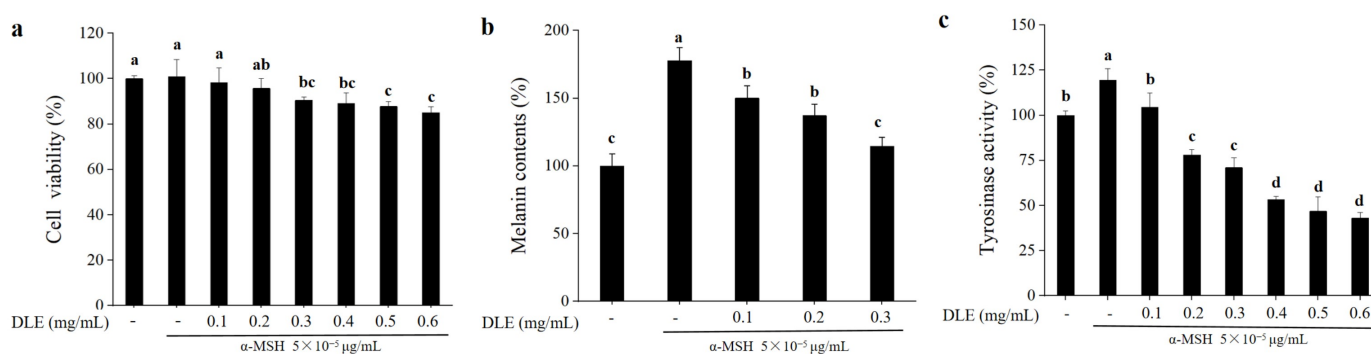


Figure 1. Effect of *Dendropanax morbifera* extract on $5 \times 10^{-5} \mu\text{g mL}^{-1}$ α -MSH-stimulated B16-F10 melanoma cells. Effect of (a) 0.1, 0.2, 0.3, 0.4, 0.5, and 0.6 mg mL^{-1} of *D. morbifera* extract on cell viability; (b) 0.1, 0.2, and 0.3 mg mL^{-1} *D. morbifera* extract on cell melanin content; (c) 0.1, 0.2, 0.3, 0.4, 0.5, and 0.6 mg mL^{-1} *D. morbifera* extract on cell tyrosinase activity. Values are represented as mean \pm S.D. Means with different letters (a–d) above the bars are significantly different by $p < 0.05$.

When B16-F10 cells were stimulated with $5 \times 10^{-5} \mu\text{g mL}^{-1}$ of α -MSH, the melanin level increased to 1.78 times that of the control. Stimulation with 0.1 to 0.3 mg mL^{-1} of *D. morbifera* extract significantly inhibited the increase in melanin level caused by α -MSH stimulation ($p < 0.05$), whereas 0.3 mg mL^{-1} of the extract produced no significant difference compared with the control group ($p > 0.05$) (Figure 1b). These results indicate that *D. morbifera* extract significantly inhibited α -MSH-stimulation-induced melanin synthesis in B16-F10 cells.

Tyrosinase activity limits melanin synthesis. We found that 0.1 mg mL^{-1} of *D. morbifera* extract inhibited the α -MSH-induced increase in tyrosinase activity and reduced it to the control level (Figure 1c). At extract concentrations >0.2 mg mL^{-1} , tyrosinase activity dropped to <75% of the control, showing a strong inhibitory effect on tyrosinase activity. These results are generally in agreement with the previous study [39].

3.3. Metabolic Profile of α -MSH-Stimulated B16-F10 Cells

To analyze the changes in cellular metabolic profiles induced by the initiation of melanin synthesis, the metabolite profiles were compared between B16-F10 cells (control group) and α -MSH-stimulated B16-F10 cells (α -MSH-stimulated groups) based on non-target metabolomics using GC-MS. In total, 79 metabolites including sugar, organic acids, fatty acids, amines, alcohols, and esters were obtained after deconvolution and identification of the raw data (Table S1). A supervised multivariate analysis, OPLS-DA, was performed to explain the differences between the control and α -MSH-stimulated groups ($R^2X = 0.858$, $R^2Y = 0.998$, $Q^2 = 0.965$). PC1 explained 28.1% of the variation, which indicates that it was a good model with a good predictive performance (Figure 2a).

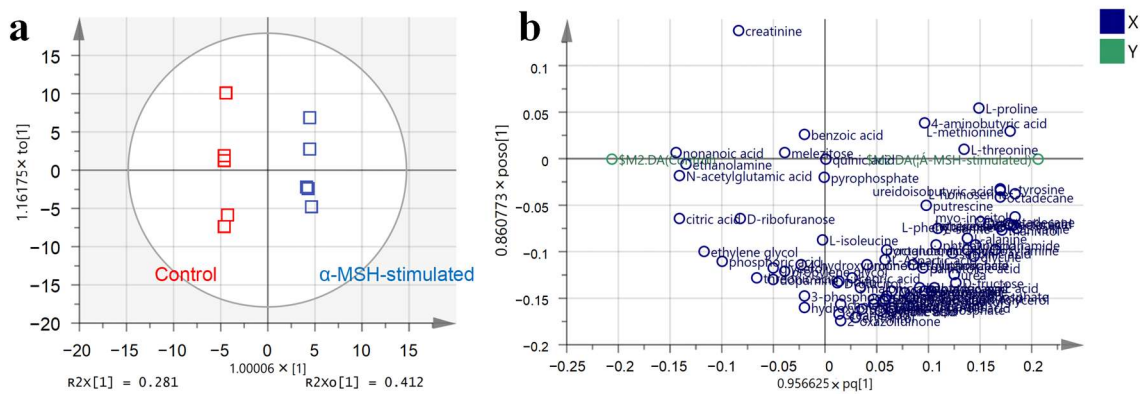


Figure 2. Orthogonal partial least squares-discriminant analysis (OPLS-DA) score (a) and loading plots (the red color represents the control group samples; the blue color represents the α -MSH-stimulated group samples) (b) of B16-F10 cells stimulated with 5×10^{-5} $\mu\text{g}/\text{mL}$ α -MSH (α -MSH-stimulated group) or not stimulated (control group).

The OPLS-DA score plots showed that the metabolite profiles of the control and α -MSH-stimulated groups were clearly separated, suggesting that α -MSH stimulation induced significant changes in the metabolic profile of B16-F10 cells (Figure 2a). The OPLS-DA loading plot showed that 20 metabolites such as nonanoic acid, citric acid, N-acetylglutamic acid, ethanolamine, ethylene glycol, phosphoric acid, creatinine, D-ribofuranose, threonic acid, glycerol, dopamine, propylene glycol, melezitose, 4-hydroxyproline, hydroxypropionic acid, and 3-phosphoglyceric acid contributed positively to PC1. In contrast, 68 metabolites contributed negatively to PC1 (Figure 2b).

Based on the results of the Student's *t*-test and VIP score of the OPLS-DA model, we selected metabolites with $p < 0.05$ and VIP score > 1 as differential metabolites (Table 2). We used MetaboAnalyst 5 to analyze the metabolomic pathways that were altered by α -MSH treatment of the B16-F10 cells (Table 3). Metabolic pathways such as phenylalanine, tyrosine, and tryptophan biosynthesis and phenylalanine metabolism affect melanin deposition in organisms [40,41]. As expected, the phenylalanine, tyrosine, and tryptophan biosynthesis metabolic pathways were significantly altered, with impact values as high as 1. This, in addition to the change in phenylalanine metabolism, suggests a significant increase in melanin synthesis levels.

Table 2. Differential metabolites between α -MSH-stimulated group and control group.

No.	Metabolites	<i>p</i> -Value	VIP Score	No.	Metabolites	<i>p</i> -Value	VIP Score
1	L-Valine	$p < 0.001$	1.440	16	propanamide	0.009	1.219
2	heneicosane	$p < 0.001$	1.419	17	L-proline	0.010	1.195
3	L-homoserine	$p < 0.001$	1.425	18	glycine	0.014	1.196
4	tetradecane	$p < 0.001$	1.391	19	citric acid	0.014	1.142
5	L-methionine	$p < 0.001$	1.378	20	L-alanine	0.020	1.130
6	lactic acid	$p < 0.001$	1.398	21	ethanolamine	0.021	1.075
7	ureidoisobutyric acid	0.001	1.319	22	nonanoic acid	0.021	1.124
8	L-phenylalanine	0.002	1.349	23	N-acetylglutamic acid	0.023	1.193
9	myo-inositol	0.002	1.419	24	hydroxylamine	0.024	1.129
10	mannitol	0.002	1.342	25	D-fructose	0.025	1.125
11	pyroglutamic acid	0.003	1.323	26	L-threonine	0.032	1.080
12	β -alanine	0.005	1.277	27	urea	0.033	1.103
13	octadecane	0.007	1.305	28	ethylene glycol	0.041	1.025
14	L-tyrosine	0.007	1.371	29	succinic acid	0.046	1.040
15	n-pentadecane	0.008	1.212				

p-Value was calculated using Student's *t*-test; variable importance in projection (VIP) score was calculated according to the orthogonal partial least squares-discriminant analysis (OPLS-DA) model.

Table 3. Differential pathways between α -MSH-stimulated group and control group.

Pathway Name	–Log (<i>p</i>)	Impact
Phenylalanine, tyrosine, and tryptophan biosynthesis	2.8812	1
Phenylalanine metabolism	1.8722	0.35714
Pantothenate and CoA biosynthesis	1.4869	0.02143
Citrate cycle (TCA cycle)	1.4451	0.12311
Glutathione metabolism	1.1784	0.09582
Glyoxylate and dicarboxylate metabolism	1.0763	0.13757
Glycine, serine, and threonine metabolism	1.0308	0.29525

p-Value and impact were calculated based on enrichment and pathway topology analysis using MetaboAnalyst.

Moreover, significant alterations were observed in other cellular metabolic pathways (Table 3), namely, pantothenate and CoA biosynthesis; citrate cycle; glutathione, glyoxylate, and dicarboxylate metabolism; and glycine, serine, and threonine metabolism. The disruption of pantothenate and CoA biosynthesis; the citrate cycle pathway; and the significant reduction in citric acid levels indicated a reduction in energy metabolism levels. The changes in the level of glutathione metabolism reflected a cellular response to stress by regulation of glutathione levels.

3.4. *D. morbifera* Extract Reversed the α -MSH-Stimulation-Induced Altered Metabolic Profile of B16-F10 Cells

B16-F10 cells were treated with different concentrations of *D. morbifera* extract (0.1, 0.2, and 0.3 mg mL^{−1}) while simultaneously stimulated with α -MSH, and the metabolite peak intensity data matrix was submitted to SIMCA 14.1 for multivariate analysis. Principal component analysis (PCA) showed aggregation among replicate samples in the same group; however, the grouping was not obvious, with $R^2X = 0.773$ and $Q^2 = 0.497$ (Figure 3a). A Q^2 value < 0.5 indicates that the model was less predictive. When OPLS-DA analysis was performed, the samples of the different groups were separated more clearly (Figure 3b), with $R^2X = 0.866$, $R^2Y = 0.924$, and $Q^2 = 0.783$, suggesting that the OPLS-DA model could better explain the experimental results with higher prediction.

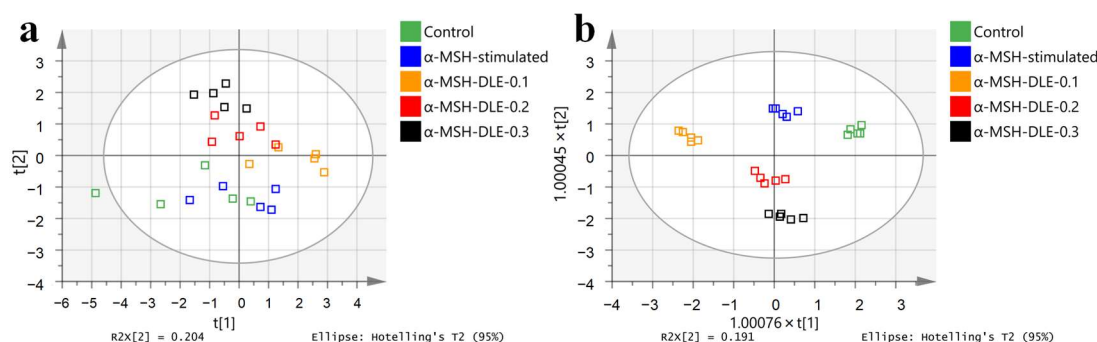


Figure 3. Multivariate analysis showing the relationship among the B16-F10 cells without any treatment (control) or treated with the addition of 0, 0.1, 0.2, 0.3 mg mL^{−1} of *D. morbifera* extract with simultaneous α -MSH stimulation. (a) Principal component analysis (PCA) score plots; (b) OPLS-DA score plots.

The Student's *t*-test showed that the levels of 25 metabolites were significantly increased because of α -MSH stimulation ($p < 0.05$) (Table 4). The addition of 0.1, 0.2, and 0.3 mg mL^{−1} of the extract reverted the level of 6, 17, and 16 metabolites, respectively, to control levels. Thus, 0.2 mg mL^{−1} of the extract exerted the strongest reversal effect on α -MSH-stimulation-induced alterations in the metabolite levels. Additionally, we noticed that the level of palmitoleic acid, which is an unsaturated fatty acid, increased further as extract concentration increased, and the level of L-tyrosine showed a 2-fold increase compared with the control group.

Table 4. Comparison among four groups of metabolites with significant difference between control and α -MSH-stimulated group based on Student's *t*-test.

Metabolites	Control	α -MSH-Stimulated	α -MSH-DLE-0.1	α -MSH-DLE-0.2	α -MSH-DLE-0.3
Metabolites upregulated by α -MSH stimulation					
octadecane	1.000 \pm 0.930	2.650 \pm 0.250 **	1.440 \pm 0.860	1.690 \pm 1.000	1.300 \pm 8.610
hydroxylamine	1.000 \pm 0.380	1.480 \pm 0.050 *	1.050 \pm 0.120	1.010 \pm 0.190	1.170 \pm 0.200
L-phenylalanine	1.000 \pm 0.170	1.470 \pm 0.190 **	1.550 \pm 0.150 **	1.080 \pm 0.160	0.950 \pm 0.140
mannitol	1.000 \pm 0.190	1.430 \pm 0.080 **	1.650 \pm 0.370 **	0.970 \pm 0.120	0.920 \pm 0.220
D-fructose	1.000 \pm 0.270	1.380 \pm 0.250 *	1.350 \pm 0.240 *	0.940 \pm 0.160	0.800 \pm 0.090
propanamide	1.000 \pm 0.210	1.380 \pm 0.210 **	0.800 \pm 0.120	1.220 \pm 0.160	1.230 \pm 0.330
pyroglutamic acid	1.000 \pm 0.130	1.360 \pm 0.170 **	1.380 \pm 0.170 **	1.140 \pm 0.140	1.120 \pm 0.090
lactic acid	1.000 \pm 0.110	1.330 \pm 0.100 **	1.340 \pm 0.170 **	1.060 \pm 0.110	1.150 \pm 0.100 *
L-Valine	1.000 \pm 0.090	1.310 \pm 0.080 **	1.200 \pm 0.120 **	0.900 \pm 0.090	0.850 \pm 0.080 *
L-methionine	1.000 \pm 0.100	1.300 \pm 0.090 **	1.340 \pm 0.190 **	0.920 \pm 0.130	0.900 \pm 0.110
urea	1.000 \pm 0.160	1.260 \pm 0.220 **	1.390 \pm 0.200 **	1.010 \pm 0.090	1.120 \pm 0.160
L-homoserine	1.000 \pm 0.070	1.260 \pm 0.080 **	1.360 \pm 0.110 **	1.090 \pm 0.120	1.080 \pm 0.150
L-threonine	1.000 \pm 0.110	1.240 \pm 0.210 *	1.310 \pm 0.180 **	0.940 \pm 0.130	0.890 \pm 0.200
n-pentadecane	1.000 \pm 0.120	1.240 \pm 0.120 **	0.930 \pm 0.120	1.070 \pm 0.070	1.170 \pm 0.220
L-proline	1.000 \pm 0.120	1.190 \pm 0.070 *	1.440 \pm 0.070 **	1.040 \pm 0.140	0.890 \pm 0.100
succinic acid	1.000 \pm 0.100	1.180 \pm 0.180 *	1.260 \pm 0.150 **	1.060 \pm 0.130	0.960 \pm 0.110
glycine	1.000 \pm 0.060	1.140 \pm 0.090 *	1.160 \pm 0.080 **	1.040 \pm 0.070	0.980 \pm 0.050
palmitoleic acid	1.000 \pm 1.390	4.140 \pm 0.780 **	7.340 \pm 0.780 **	8.000 \pm 0.990 **	9.700 \pm 0.880 **
L-tyrosine	1.000 \pm 1.010	2.740 \pm 0.680 **	3.700 \pm 0.620 **	2.100 \pm 0.540 *	2.060 \pm 0.450 *
heneicosane	1.000 \pm 0.160	1.570 \pm 0.150 **	0.970 \pm 0.110	1.170 \pm 0.070 *	1.210 \pm 0.180 *
tetradecane	1.000 \pm 0.180	1.560 \pm 0.150 **	1.000 \pm 0.120	1.190 \pm 0.100 *	1.270 \pm 0.160 *
myo-inositol	1.000 \pm 0.080	1.460 \pm 0.190 **	1.400 \pm 0.150 **	1.140 \pm 0.140 *	0.980 \pm 0.090 *
ureidoisobutyric acid	1.000 \pm 0.090	1.230 \pm 0.080 **	1.300 \pm 0.140 **	1.210 \pm 0.070 **	0.970 \pm 0.060
β -alanine	1.000 \pm 0.080	1.160 \pm 0.070 **	1.320 \pm 0.100 **	1.130 \pm 0.110 *	1.110 \pm 0.090 *
L-alanine	1.000 \pm 0.040	1.080 \pm 0.060 *	1.060 \pm 0.050 *	0.920 \pm 0.060 *	0.850 \pm 0.070 **
Metabolites downregulated by α -MSH stimulation					
ethylene glycol	1.000 \pm 0.040	0.950 \pm 0.030 *	0.980 \pm 0.040	0.940 \pm 0.040 *	0.910 \pm 0.050 **
citric acid	1.000 \pm 0.210	0.690 \pm 0.150 *	1.040 \pm 0.220	1.320 \pm 0.150 **	1.340 \pm 0.190 **
ethanolamine	1.000 \pm 0.210	0.640 \pm 0.250 *	1.110 \pm 0.310	0.630 \pm 0.140 **	0.530 \pm 0.120 **
nonanoic acid	1.000 \pm 0.270	0.580 \pm 0.280 *	0.400 \pm 0.030 **	0.550 \pm 0.190 **	0.410 \pm 0.050 **
N-acetylglutamic acid	1.000 \pm 0.340	0.580 \pm 0.090 *	0.470 \pm 0.070 *	0.580 \pm 0.100 *	0.470 \pm 0.020 *
benzoic acid	1.000 \pm 0.150	0.400 \pm 0.550 *	0.940 \pm 0.070	0.980 \pm 0.140	0.760 \pm 0.440

* Indicates when the group is compared with the control, $p < 0.05$; ** indicates when the group is compared with the control, $p < 0.01$.

The levels of six metabolites, namely, ethylene glycol, citric acid, ethanolamine, nonanoic acid, N-acetylglutamic acid, and benzoic acid, decreased in B16-F10 cells following α -MSH stimulation (Table 4). Notably, an addition of 0.1 mg mL⁻¹ of extract reverted the citric acid level to that of the control ($p > 0.05$), whereas an addition of 0.2 and 0.3 mg mL⁻¹ of extract produced a 1.3-fold increase in citric acid levels compared with the control. These results suggested that the addition of *D. morbifera* extract was effective in improving energy metabolism.

Hierarchical cluster analysis (HCA) was performed to visualize the difference in metabolite profiles among the different treatment groups. A heatmap showed that metabolite abundances changed significantly after α -MSH stimulation. The cellular metabolite profiles were similar between the α -MSH-stimulated group and α -MSH-DLE-0.1 group, whereas the metabolite profiles of the α -MSH-DLE-0.2 group were similar to those of the control group (Figure 4). Thus, the combined results of the multivariate analysis, *t*-test, and HCA analysis show that 0.2 mg mL⁻¹ of the extract is more effective than other concentrations in reverting the effect of α -MSH stimulation.

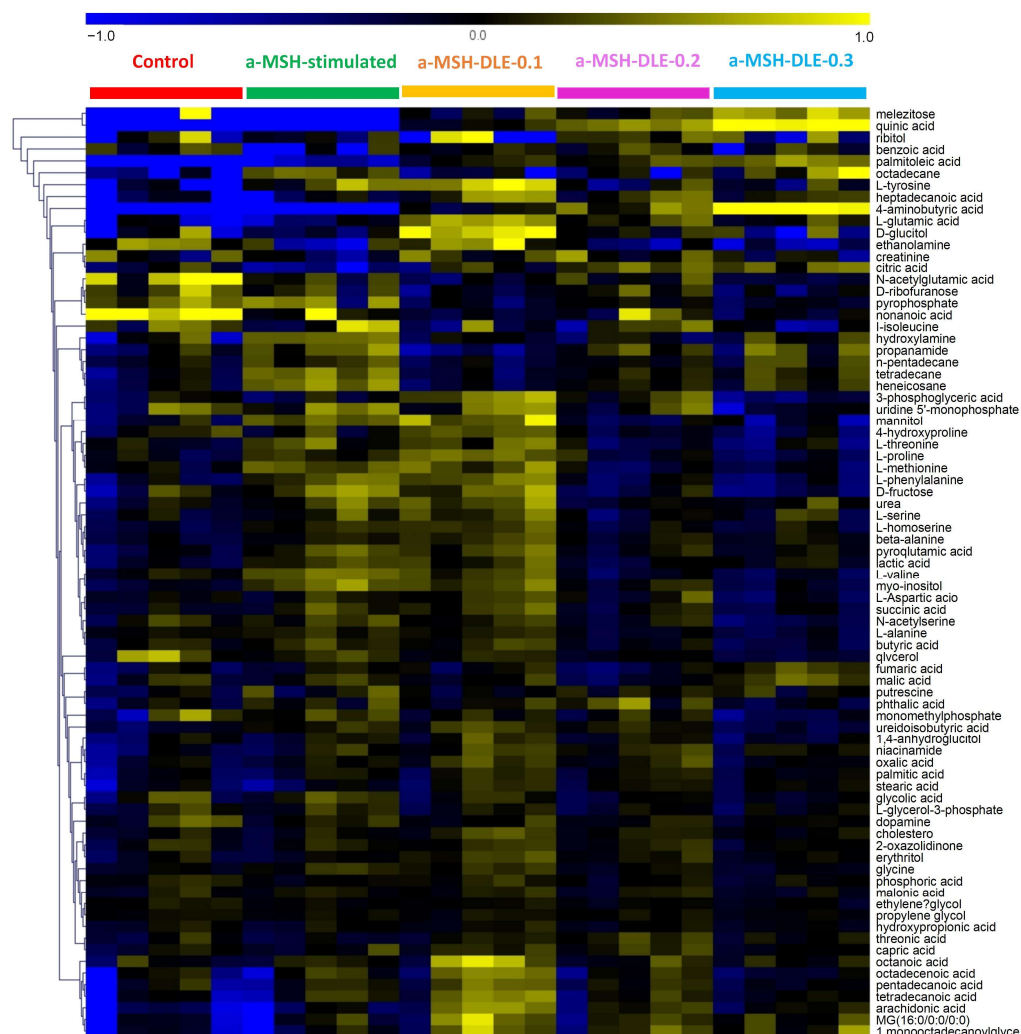


Figure 4. Hierarchical cluster analysis (HCA) of 79 metabolites in B16-F10 cells under different treatments. Cluster similarity was assessed based on the Pearson correlation coefficient and the average linkage method. Each vertical column represents a sample, and each horizontal row represents a different metabolite.

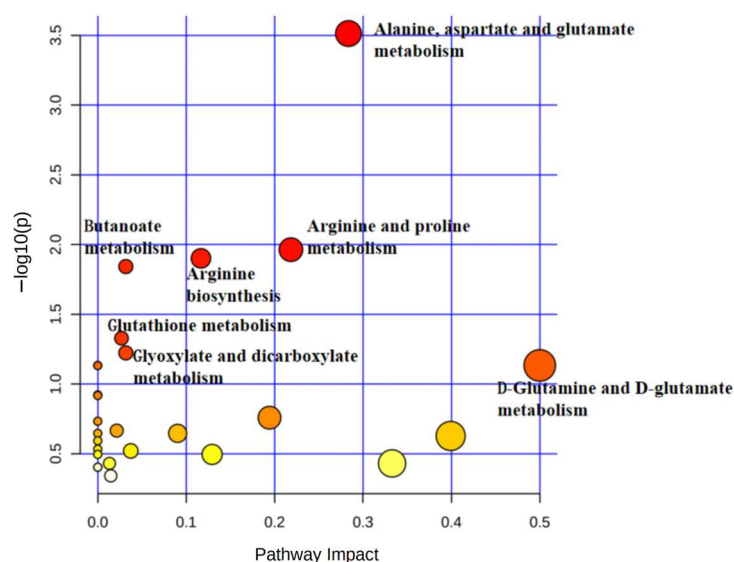
3.5. Treatment of α -MSH-Stimulated B16-F10 Cells with *D. morbifera* Extract Showed Metabolic Differences Compared with the Control

To evaluate other biological effects of α -MSH stimulation in B16-F10 cells when stimulated with 0.2 mg mL^{-1} of *D. morbifera* extract, we established an OPLS-DA model ($R^2X = 0.846$, $R^2Y = 0.997$, and $Q^2 = 0.958$; data shown in Figure S1). Based on the Student's *t*-test results, metabolites with $p < 0.05$ and VIP score > 1 were selected as differential metabolites (Table 5), and the possible alterations to metabolic pathways were analyzed (Figure 5).

Compared with those of the control group, the levels of 25 metabolites including palmitoleic acid, 4-aminobutyric acid, ureidoisobutyric acid, niacinamide, arachidonic acid, citric acid, L-glutamic acid, and eptadecanoic acid significantly increased. The levels of five metabolites, namely, ethanolamine, nonanoic acid, pyrophosphate, N-acetylglutamic acid, and ethylene glycol significantly decreased (Table 5).

Table 5. Differential metabolites between control and α -MSH-DLE-0.2 groups ($p < 0.05$ and VIP score > 1).

No.	Metabolites	p -Value	VIP Score	No.	Metabolites	p -Value	VIP Score
Metabolites upregulated by α -MSH-DLE-0.2							
1	palmitoleic acid	$p < 0.001$	1.193	11	phthalic acid	0.026	1.138
2	4-aminobutyric acid	$p < 0.001$	1.675	12	β -alanine	0.035	1.124
3	ureidoisobutyric acid	0.002	1.422	13	tetradecane	0.038	1.153
4	niacinamide	0.006	1.367	14	putrescine	0.038	1.121
5	arachidonic acid	0.011	1.244	15	heneicosane	0.039	1.166
6	citric acid	0.012	1.283	16	MG (16:0/0:0/0:0)	0.041	1.119
7	L-glutamic acid	0.014	1.246	17	myo-inositol	0.042	1.139
8	heptadecanoic acid	0.022	1.529	18	palmitic acid	0.045	1.131
9	L-alanine	0.025	1.208	19	threonic acid	0.046	1.122
10	1-monooctadecanoylglycerol	0.025	1.183	20	oxalic acid	0.047	1.145
Metabolites downregulated by α -MSH-DLE-0.2							
21	ethanolamine	0.007	1.352	24	N-acetylglutamic acid	0.024	1.275
22	nonanoic acid	0.008	1.338	25	ethylene glycol	0.030	1.165
23	pyrophosphate	0.014	1.391				

**Figure 5.** Pathway analysis using MetaboAnalyst 5. The color and size of the circles indicates their p -value and pathway impact value, respectively. The pathway impact (X -axis) and $-\log p$ -value (Y -axis) were calculated using pathway topology analysis and pathway enrichment analysis, respectively. Alanine, aspartate, and glutamate metabolism; arginine and proline metabolism; arginine biosynthesis; butanoate metabolism; glutathione metabolism; and glyoxylate and dicarboxylate metabolism were significantly different between the α -MSH-DLE-0.2 group and control group (without any treatment) at a significance level of $p < 0.01$ with adjusted false discovery rate (FDR) $p < 0.05$.

Treating α -MSH-stimulated B16-F10 cells with and 0.2 mg mL^{-1} of *D. morbifera* extract resulted in niacinamide accumulation. This is a significant finding because in a previous study, Li et al. [42] proved that niacinamide could potentially stabilize the dual anti-melanin effect of rhizobium nanocrystals in zebrafish larvae. Thus, the accumulation of niacinamide in B16-F10 cells suggests the possible inhibition of melanin production.

These differential metabolites are involved in alanine, aspartate, and glutamate metabolism; arginine and proline metabolism; arginine biosynthesis; butanoate metabolism; glutathione metabolism; and glyoxylate and dicarboxylate metabolism (Figure 5). Moreover, the results of the current study are consistent with those of a previous study, which reported that alterations in arginine and proline metabolism; alanine metabolism; aspartate metabolism; glutamate metabolism; and glutathione metabolism altered melanin production [43].

These results were consistent with those of previous studies that state that glutathione metabolism is involved in regulating melanin biosynthesis [44,45]. During glutathione synthesis, cysteine is combined with glutamate, to which glycine is added [46]. In this study, the levels of glutamate and glycine, which were related to glutathione biosynthesis, increased in response to the *D. morbifera* extract, indicating the activation of glutathione biosynthesis and decreased melanin synthesis.

The enhancement of arginine biosynthesis promotes the accumulation of arginine, which is decomposed into citrulline and nitric oxide (NO) by the action of nitric oxide synthase (NOS) [47]. NO causes the self-destruction of melanocytes, leading to skin depigmentation [48]. The level of urea generated from arginine increased compared with that of the control following α -MSH stimulation, whereas the levels were the same as those of the control following treatment with *D. morbifera* extract. Therefore, we speculated that NO production may occur, which enhances the antioxidant capacity of cells to cope with stress response.

Although the previous study reported the inhibition of tyrosinase activity and melanin formation by *D. morbifera* Leveille extract in α -MSH-induced B16-F10 cells, with a focus on the active ingredients [40], this study delves deeper into the metabolic changes induced by the extract, which is a novel approach that has not been explored in previous studies. In further studies, we plan to investigate the whitening effect of specific bioactive compounds isolated from *D. morbifera* Leveille extract to better understand their contributions to melanin inhibition.

4. Conclusions

To the best of our knowledge, this is the first study to evaluate the whitening effects of *D. morbifera* extract and elucidate the alteration in metabolite profile with the aim of providing comprehensive insights into the metabolic changes and mechanisms associated with melanin synthesis.

D. morbifera extract showed low cytotoxicity and good melanin production inhibiting capacity. OPLS-DA and HCA analyses showed a significant difference in the metabolite profiles of the control, α -MSH stimulation, and *D. morbifera* extract treatment groups. The levels of 30 metabolites including palmitoleic acid, 4-aminobutyric acid, ureidoisobutyric acid, niacinamide, and L-glutamic acid changed in B16-F10 cells following treatment with *D. morbifera* extract. These metabolites were related to melanin-biosynthesis-associated pathways, namely, alanine, aspartate, and glutamate metabolism; arginine and proline metabolism; arginine biosynthesis; and glutathione metabolism.

D. morbifera extract reversed the alterations induced in the B16-F10 cellular metabolite profile by α -MSH stimulation, restored the metabolite levels to those of the control, and downregulated melanin-synthesis-associated pathways. Additionally, metabolic analysis demonstrated that *D. morbifera* extract promotes energy metabolism, enhances antioxidant-related signaling pathways, and reduces the level of melanin-synthesis-related pathways. These results demonstrate that *D. morbifera* extract can be used as a potential melanin inhibitor for the development of whitening cosmetics. However, additional research is necessary to comprehensively understand the mechanisms underlying these effects and establish optimal dosage and formulation for maximum efficacy.

Supplementary Materials: The following supporting information can be downloaded at: <https://www.mdpi.com/article/10.3390/horticulturae10030219/s1>, Figure S1: (a) OPLS-DA score and (b) loading plots of B16 cells stimulated with 5×10^{-5} $\mu\text{g}/\text{mL}$ α -MSH and 0.2 mg/mL *Dendropanax morbifera* Leveille extract (α -MSH-DLE-0.2) or control; Table S1: Identified metabolites extracted from B16-F10 cells.

Author Contributions: Conceptualization, T.B. and S.K.; methodology, T.B.; software, T.B.; validation, T.B., D.K. and S.K.; formal analysis, T.B.; investigation, D.K. and S.K.; resources, S.K.; data curation, D.K. and S.K.; writing—original draft preparation, T.B., D.K. and S.K.; writing—review and editing,

D.K. and S.K.; visualization, T.B.; supervision, S.K.; project administration, D.K. and S.K.; funding acquisition, S.K. All authors have read and agreed to the published version of the manuscript.

Funding: This study was supported by a National Research Foundation of Korea (NRF) grant funded by the Korean government (MSIT) (No. 2022R1F1A1071270).

Data Availability Statement: Data are contained within the article and Supplementary Materials.

Conflicts of Interest: The authors declare no conflicts of interest.

References

1. Biyashev, D.; Siwicka, Z.E.; Onay, U.V.; Demczuk, M.; Xu, D.; Ernst, M.K.; Evans, S.T.; Nguyen, C.V.; Son, F.A.; Paul, N.K.; et al. Topical application of synthetic melanin promotes tissue repair. *NPJ Regen. Med.* **2023**, *8*, 61–74. [[CrossRef](#)]
2. Díaz, D.F.Z.; Busch, L.; Kröger, M.; Klein, A.L.; Lohan, S.B.; Mewes, K.R.; Vierkotten, L.; Witzel, C.; Rohn, S.; Meinke, M.C. Significance of melanin distribution in the epidermis for the protective effect against UV light. *Sci. Rep.* **2024**, *14*, 3488. [[CrossRef](#)]
3. Matoba, Y.; Kihara, S.; Bando, N.; Yoshitsu, H.; Sakaguchi, M.; Kayama, K.; Yanagisawa, S.; Ogura, T.; Sugiyama, M. Catalytic mechanism of the tyrosinase reaction toward the Tyr⁹⁸ residue in the caddie protein. *PLoS Biol.* **2018**, *16*, e3000077–e3000098. [[CrossRef](#)]
4. Zhao, Y.; Zhang, T.R.; Ning, Y.Z.; Wang, D.; Li, F.; Fan, Y.P.; Yao, J.Y.; Ren, G.Y.; Zhang, B. Identification and molecular mechanism of novel tyrosinase inhibitory peptides from the hydrolysate of ‘Fengdan’ peony (*Paeonia ostii*) seed meal proteins: Peptidomics and in silico analysis. *LWT-Food Sci. Technol.* **2023**, *180*, 114695–114704. [[CrossRef](#)]
5. D’Mello, S.A.N.; Finlay, G.J.; Baguley, B.C.; Askarian-Amiri, M.E. Signaling pathways in melanogenesis. *Int. J. Mol. Sci.* **2016**, *17*, 1144. [[CrossRef](#)] [[PubMed](#)]
6. Lee, S.E.; Park, S.H.; Oh, S.W.; Yoo, J.A.; Kwon, K.; Park, S.J.; Kim, J.; Lee, H.S.; Cho, J.Y.; Lee, J. Beauvericin inhibits melanogenesis by regulating cAMP/PKA/CREB and LXR- α /p38 MAPK-mediated pathways. *Sci. Rep.* **2018**, *8*, 14958–14969. [[CrossRef](#)] [[PubMed](#)]
7. Bourhim, T.; Villareal, M.O.; Gadhi, C.; Isoda, H. Elucidation of melanogenesis-associated signaling pathways regulated by argan press cake in B16 melanoma cells. *Nutrients* **2021**, *13*, 2697. [[CrossRef](#)] [[PubMed](#)]
8. Liu-Smith, F.; Meyskens, F.L. Molecular mechanisms of flavonoids in melanin synthesis and the potential for the prevention and treatment of melanoma. *Mol. Nutr. Food Res.* **2016**, *60*, 1264–1274. [[CrossRef](#)] [[PubMed](#)]
9. Sattar, M.A.; Patnaik, A. Molecular insights into antioxidant efficiency of melanin: A sustainable antioxidant for natural rubber formulations. *J. Phys. Chem. B* **2023**, *127*, 8242–8256. [[CrossRef](#)] [[PubMed](#)]
10. Lu, Y.; Xu, Y.; Song, M.T.; Qian, L.L.; Liu, X.L.; Gao, R.Y.; Han, R.M.; Skibsted, L.H.; Zhang, J.P. Promotion effects of flavonoids on browning induced by enzymatic oxidation of tyrosinase: Structure-activity relationship. *RSC Adv.* **2021**, *11*, 13769–13779. [[CrossRef](#)] [[PubMed](#)]
11. Monmai, C.; Kim, J.S.; Chin, J.H.; Lee, S.H.Y.; Baek, S.H. Inhibitory effects of polyphenol- and flavonoid-enriched rice seed extract on melanogenesis in melan-a cells via MAPK signaling-mediated MITF downregulation. *Int. J. Mol. Sci.* **2023**, *24*, 11841. [[CrossRef](#)]
12. Wang, Y.; Yu, J.; Chen, Y.K.; Wang, Z.C. Complete chloroplast genome sequence of the endemic and endangered plant *Dendropanax oligodontus*: Genome structure, comparative and phylogenetic analysis. *Genes* **2022**, *13*, 2028. [[CrossRef](#)] [[PubMed](#)]
13. Hyun, T.K.; Ko, Y.-J.; Kim, E.-H.; Chung, I.-M.; Kim, J.-S. Anti-inflammatory activity and phenolic composition of *Dendropanax morbifera* leaf extracts. *Ind. Crop. Prod.* **2015**, *74*, 263–270. [[CrossRef](#)]
14. Youn, J.S.; Kim, Y.-J.; Na, H.J.; Jung, H.R.; Song, C.K.; Kang, S.Y.; Kim, J.Y. Antioxidant activity and contents of leaf extracts obtained from *Dendropanax morbifera* LEV are dependent on the collecting season and extraction conditions. *Food Sci. Biotechnol.* **2019**, *28*, 201–207. [[CrossRef](#)] [[PubMed](#)]
15. Zhang, M.; Bu, T.; Liu, S.; Kim, S. Optimization of caffeic acid extraction from *Dendropanax morbifera* leaves using response surface methodology and determination of polyphenols and antioxidant properties. *Horticulturae* **2021**, *7*, 491. [[CrossRef](#)]
16. Lee, J.-Y.; Park, T.-H.; Park, S.-H.; Yang, S.-A.; Jhee, K.-H. The antimicrobial activity of fermented extracts from Korean *Dendropanax morbifera*. *J. Life Sci.* **2019**, *29*, 29–36.
17. Moon, H.-I. Antidiabetic effects of dendropanoxide from leaves of *Dendropanax morbifera* Leveille in normal and streptozotocin-induced diabetic rats. *Hum. Exp. Toxicol.* **2011**, *30*, 870–875. [[CrossRef](#)] [[PubMed](#)]
18. An, N.Y.; Kim, J.-E.; Hwang, D.; Ryu, H.K. Anti-diabetic effects of aqueous and ethanol extract of *Dendropanax morbifera* Leveille in streptozotocin-induced diabetes model. *J. Nutr. Health* **2014**, *47*, 394–402. [[CrossRef](#)]
19. Wang, C.; Mathiyalagan, R.; Kim, Y.J.; Castro-Aceituno, V.; Singh, P.; Ahn, S.; Wang, D.; Yang, D.C. Rapid green synthesis of silver and gold nanoparticles using *Dendropanax morbifera* leaf extract and their anticancer activities. *Int. J. Nanomed.* **2016**, *11*, 3691.
20. Bae, D.; Kim, J.; Lee, S.Y.; Choi, E.J.; Jung, M.A.; Jeong, C.S.; Na, J.R.; Kim, J.J.; Kim, S. Hepatoprotective effects of aqueous extracts from leaves of *Dendropanax morbifera* leveille against alcohol-induced hepatotoxicity in rats and in vitro anti-oxidant effects. *Food Sci. Biotechnol.* **2015**, *24*, 1495–1503. [[CrossRef](#)]
21. Park, B.-Y.; Min, B.-S.; Oh, S.-R.; Kim, J.-H.; Kim, T.-J.; Kim, D.-H.; Bae, K.-H.; Lee, H.-K. Isolation and anticomplement activity of compounds from *Dendropanax morbifera*. *J. Ethnopharmacol.* **2004**, *90*, 403–408. [[CrossRef](#)] [[PubMed](#)]

22. Lee, S.-H.; Lee, H.-S.; Park, Y.-S.; Hwang, B.; Kim, J.-H.; Lee, H.-Y. Screening of immune activation activities in the leaves of *Dendropanax morbifera* Lev. *Korean J. Med. Crop Sci.* **2002**, *10*, 109–115.
23. Park, Y.J.; Kim, D.M.; Choi, H.B.; Jeong, M.H.; Kwon, S.H.; Kim, H.; Kwak, J.H.; Chung, K.H. Dendropanoxide, a triterpenoid from *Dendropanax morbifera*, ameliorates hepatic fibrosis by inhibiting activation of hepatic stellate cells through autophagy inhibition. *Nutrients* **2022**, *14*, 98. [[CrossRef](#)] [[PubMed](#)]
24. Chung, I.M.; Kim, S.H.; Kwon, C.; Kim, S.Y.; Yang, Y.J.; Kim, J.S.; Ali, M.; Ahmad, A. New chemical constituents from the bark of *Dendropanax morbifera* Leveille and their evaluation of antioxidant activities. *Molecules* **2019**, *24*, 3967. [[CrossRef](#)] [[PubMed](#)]
25. Lee, J.W.; Ryu, H.W.; Lee, S.U.; Son, T.H.; Park, H.A.; Kim, M.O.; Yuk, H.J.; Ahn, K.S.; Oh, S.R. Protective effect of polyacetylene from *Dendropanax morbifera* Leveille leaves on pulmonary inflammation induced by cigarette smoke and lipopolysaccharide. *J. Funct. Foods* **2017**, *32*, 358–366. [[CrossRef](#)]
26. Kim, M.; Park, Y.J.; Lim, H.-S.; Lee, H.-H.; Kim, T.-H.; Lee, B. The clinical effects of *Dendropanax morbifera* on postmenopausal symptoms. *J. Menopausal Med.* **2017**, *23*, 146–155. [[CrossRef](#)]
27. Yang, H.Y.; Kim, K.S.; Lee, Y.H.; Park, J.H.; Kim, J.H.; Lee, S.Y.; Kim, Y.M.; Kim, I.S.; Kacew, S.; Lee, B.M.; et al. *Dendropanax morbifera* ameliorates thioacetamide-induced hepatic fibrosis via TGF- β 1/Smads pathways. *Int. J. Biol. Sci.* **2019**, *15*, 800–811. [[CrossRef](#)]
28. Shin, D.-C.; Kim, G.-C.; Song, S.-Y.; Kim, H.-J.; Yang, J.-C.; Kim, B.-A. Antioxidant and antiaging activities of complex supercritical fluid extracts from *Dendropanax morbifera*, *Corni fructus* and *Lycii fructus*. *Korea J. Herbol.* **2013**, *28*, 95–100. [[CrossRef](#)]
29. Hoang, H.T.; Park, J.S.; Kim, S.H.; Moon, J.Y.; Lee, Y.C. Microwave-assisted *Dendropanax morbifera* extract for cosmetic applications. *Antioxidants* **2022**, *11*, 998. [[CrossRef](#)]
30. Lee, K.Y.; Jung, H.Y.; Yoo, D.Y.; Kim, W.; Kim, J.W.; Kwon, H.J.; Kim, D.W.; Yoon, Y.S.; Hwang, I.K.; Choi, J.H. *Dendropanax morbifera* Léveille extract ameliorates D-galactose-induced memory deficits by decreasing inflammatory responses in the hippocampus. *Lab Anim. Res.* **2017**, *33*, 283–290. [[CrossRef](#)]
31. Choo, G.S.; Lim, D.P.; Kim, S.M.; Yoo, E.S.; Kim, S.H.; Kim, C.H.; Woo, J.S.; Kim, H.J.; Jung, J.Y. Anti-inflammatory effects of *Dendropanax morbifera* in lipopolysaccharide-stimulated RAW264.7 macrophages and in an animal model of atopic dermatitis. *Mol. Med. Rep.* **2019**, *19*, 2087–2096. [[CrossRef](#)]
32. Chen, Y.; Wang, M.; Li, X. Positive significance of confucianism on moral construction of college counselors. *Chin. Med. J.* **2015**, 517–519.
33. Roshanak, S.; Rahimmalek, M.; Goli, S.A.H. Evaluation of seven different drying treatments in respect to total flavonoid, phenolic, vitamin C content, chlorophyll, antioxidant activity and color of green tea (*Camellia sinensis* or *C. assamica* leaves). *J. Food Sci. Technol.* **2016**, *53*, 721–729. [[CrossRef](#)]
34. Masson, P.; Spagou, K.; Nicholson, J.K.; Want, E.J. Technical and biological Variation in UPLC–MS-based untargeted metabolic profiling of liver extracts: Application in an experimental toxicity study on galactosamine. *Anal. Chem.* **2011**, *83*, 1116–1123. [[CrossRef](#)]
35. Davies, T. The new automated mass spectrometry deconvolution and identification system (AMDIS). *Spectrosc. Eur.* **1998**, *10*, 24–27.
36. Styczynski, M.P.; Moxley, J.F.; Tong, L.V.; Walther, J.L.; Jensen, K.L.; Stephanopoulos, G.N. Systematic identification of conserved metabolites in GC/MS data for metabolomics and biomarker discovery. *Anal. Chem.* **2007**, *79*, 966–973. [[CrossRef](#)]
37. Carvalho, T.G.C.; dos Santos, I.M.; Bedor, C.N.G.; de Alencar, E.B. Principal component analysis (PCA) and construction of a SIMCA classification model to monoterpenes and analogs with larvicidal activity in *Aedes aegypti*. *Rev. Virtual Quim.* **2019**, *11*, 411–424. [[CrossRef](#)]
38. Agbo, M.; Uzor, P.; Akazie-Nneji, U.; Eze-Odurukwe, C.; Ogbatue, U.; Mbaaji, E. Antioxidant, total phenolic and flavonoid content of selected Nigerian medicinal plants. *Dhaka Univ. J. Pharm. Sci.* **2015**, *14*, 35–41. [[CrossRef](#)]
39. Park, J.U.; Yang, S.Y.; Guo, R.H.; Li, H.X.; Kim, Y.H.; Kim, Y.R. Anti-melanogenic effect of *Dendropanax morbiferus* and its active components via protein kinase A/Cyclic adenosine monophosphate-responsive binding protein- and p38 mitogen-activated protein kinase-mediated microphthalmia-associated transcription factor downregulation. *Front. Pharmacol.* **2020**, *11*, 507–516. [[CrossRef](#)] [[PubMed](#)]
40. Bu, T.; Zhang, M.; Lee, S.-H.; Cheong, Y.E.; Park, Y.; Kim, K.H.; Kim, D.; Kim, S. GC-TOF/MS-based metabolomics for comparison of volar and non-volar skin types. *Metabolites* **2022**, *12*, 717. [[CrossRef](#)] [[PubMed](#)]
41. Ahmad, S.; Mohammed, M.; Mekala, L.P.; Chintalapati, S.; Chintalapati, V.R. Tryptophan, a non-canonical melanin precursor: New L-tryptophan based melanin production by *Rubrivivax benzoatilyticus* JA2. *Sci. Rep.* **2020**, *10*, 8925–8936. [[CrossRef](#)] [[PubMed](#)]
42. Li, Y.; Xiang, H.; Xue, X.; Chen, Y.; He, Z.; Yu, Z.; Zhang, L.; Miao, X. Dual antimelanogenic effect of nicotinamide-stabilized phloretin nanocrystals in larval zebrafish. *Pharmaceutics* **2022**, *14*, 1825. [[CrossRef](#)] [[PubMed](#)]
43. Marzabani, R.; Rezadoost, H.; Choopanian, P.; Kolahdoost, S.; Mozafari, N.; Mirzaie, M.; Karimi, M.; Nieminen, A.I.; Jafari, M. Metabolomic signature of amino acids in plasma of patients with non-segmental Vitiligo. *Metabolomics* **2021**, *17*, 92–102. [[CrossRef](#)] [[PubMed](#)]
44. Jeon, G.; Kim, C.; Cho, U.M.; Hwang, E.T.; Hwang, H.S.; Min, J. Melanin-decolorizing activity of antioxidant enzymes, glutathione peroxidase, thiol peroxidase, and catalase. *Mol. Biotechnol.* **2021**, *63*, 150–155. [[CrossRef](#)]
45. Boo, Y.C. Metabolic basis and clinical evidence for skin lightening effects of thiol compounds. *Antioxidants* **2022**, *11*, 503. [[CrossRef](#)]
46. Lu, S.C. Glutathione synthesis. *Biochim. Biophys. Acta* **2013**, *1830*, 3143–3153. [[CrossRef](#)]

47. Flam, B.R.; Eichler, D.C.; Solomonson, L.P. Endothelial nitric oxide production is tightly coupled to the citrulline-NO cycle. *Nitric Oxide-Biol. Chem.* **2007**, *17*, 115–121. [[CrossRef](#)]
48. Marek, L.; Tam, I.; Kurkiewicz, S.; Dzierzega-Leczna, A. The pigmentation phenotype of melanocytes affects their response to nitric oxide in vitro. *Postepy Dermatol. Alergol.* **2023**, *40*, 150–158. [[CrossRef](#)]

Disclaimer/Publisher’s Note: The statements, opinions and data contained in all publications are solely those of the individual author(s) and contributor(s) and not of MDPI and/or the editor(s). MDPI and/or the editor(s) disclaim responsibility for any injury to people or property resulting from any ideas, methods, instructions or products referred to in the content.